Stochastic Geometry-based Analysis of the Distribution of Peak Age of Information

Praful D. Mankar, Mohamed A. Abd-Elmagid, and Harpreet S. Dhillon

***Abstract*—In this paper, we consider a large-scale wireless network consisting of source-destination (SD) pairs where the source nodes frequently send status updates about some underlying physical processes (observed by them) to their corresponding destination nodes. For this setup, we employ age of information (AoI) as a performance metric to quantify freshness of the status updates when they reach the destination nodes. While most of the existing works are focused on the analysis of the temporal mean AoI in deterministic network topologies, we aim to characterize the spatial AoI performance disparity that is inherently present in wireless networks. In particular, we treat the temporal mean AoI as a random variable over space as the update delivery rate of a wireless link is a function of the interference field observed by its receiver. Our objective is to characterize the spatial distribution of the temporal mean AoI observed by the SD pairs by modeling them as a Poisson bipolar process. We first derive accurate bounds on the moments of the successful transmission probability of a status update which are then used to derive tight bounds on the moments as well as the spatial distribution of the temporal mean peak AoI. Our results provide useful design guidelines on the appropriate selection of different system parameters to minimize the mean peak AoI.**

***Index Terms*—Age of information, meta distribution, stochastic geometry, and wireless networks.**

I. Introduction

Popular performance metrics used in communication system design, such as throughput and delay, lack the ability of quantifying the freshness of data packets transmitted from source nodes, e.g., the Internet of Things (IoT) devices, to the destination nodes, such as cellular base stations. This has recently motivated the use of AoI to quantify the performance of communication systems that deal with time-sensitive information [2]. This metric was first introduced in [3] for a simple queueing-theoretic model for which the temporal mean AoI was characterized. Although it is more meaningful to characterize the distribution of AoI, the subsequent works were mostly focused on characterizing the temporal mean of AoI or other age-related metrics (e.g., peak AoI and Value of Information of Update) for various system settings in [3] to maintain analytical tractability (refer to [4] for a detailed discussion). While these queueing theory-based works provided foundational understanding of AoI, their setting is not conducive to account for some key characteristics of wireless networks, such as interference, temporal channel variations and random spatial distribution of nodes. Because of this, their analyses cannot account for the spatial disparity in the AoI experienced by the wireless links spread across the network. Inspired by this, we develop a novel analytical framework with foundations in stochastic geometry that facilitates spatio-temporal analysis of AoI, resulting in new results on the spatial distribution of the temporal mean peak AoI.

Related work. AoI has been extensively used as a performance metric for a variety of wireless communications networks, including broadcast networks [5], [6], multicast networks [7], radio frequency-powered networks [8], ultra-reliable low-latency vehicular networks [9], and unmanned aerial vehicle (UAV)-assisted networks [10], [11]. Recalling that the main objective of this paper is the analysis of the spatial distribution of the temporal mean peak AoI in wireless network, the most relevant literature can be categorized into two sets: i) the analysis of distribution of AoI, and ii) applications of stochastic geometry for AoI analysis, which are briefly discussed next.

The temporal distribution of AoI has been analyzed in [12]–[15] from a queueing-theoretic perspective for a single SD pair. The authors of [12] ([15]) characterized the distribution of AoI for a continuous (discrete) time queue with an infinite capacity while considering a first-come-first-served queueing discipline. The distribution of AoI for queuing systems with no queue or a unit capacity queue was derived in [13] under non-preemptive scheduling. The authors of [14] obtained the probability mass function (`pmf`) of AoI for a multi-hop network with time-invariant packet loss probabilities on each link.

Owing to their analytical tractability and realism, stochastic geometry models have been extensively used for the analysis of large-scale wireless networks (refer to [16]). However, the inclusion of explicit temporal dimension in stochastic geometry-based models is known to be hard for the analysis of traffic aware metrics, such as delay and AoI. As a result, while there are a handful of recent works focusing on the application of stochastic geometry to AoI [17]–[20], their scope is limited to the analysis of the spatio-temporal mean of AoI [17] or peak AoI [18], [19], which fail to capture the spatial disparity in temporal mean AoI.

Contributions. Our main contribution is the analytical characterization of the spatial distribution of the temporal mean peak AoI in a large-scale wireless network in which the locations of the SD pairs follow a bipolar Poisson point process (PPP). To handle the interference-induced coupling across queues associated with SD pairs, we propose a two-step analytical framework which relies on a careful construction of *dominant systems*. Using this framework, we derive tight lower bounds on the moments of the conditional success probability of transmitting a status update using which we obtain

P. D. Mankar is with SPCRC, IIIT Hyderabad, India (Email: praful.mankar@iiit.ac.in). M. A. Abd-Elmagid and H. S. Dhillon are with Wireless@VT, Department of ECE, Virginia Tech, Blacksburg, VA (Email: {maelaziz, hdhillon}@vt.edu). The support of IIIT Hyderabad, India and U.S. NSF (Grant CPS-1739642) is gratefully acknowledged. Please refer to [1] for an expanded version of this article.

an approximate, yet accurate, distribution of the conditional success probability. Afterwards, these results are then used to derive bounds on the moments and distribution of the conditional (temporal) mean peak AoI. Our numerical results verify the analytical findings and demonstrate the impact of system design parameters on the conditional mean peak AoI.

II. System Model

We model the SD pairs using a Poisson bipolar model wherein the locations of sources follow PPP Φ with density $\lambda_{\rm sd}$ and their corresponding destinations are located at fixed distance R in uniformly random directions. By the virtue of Slivnyak's theorem, we know that conditioning on a point is the same as adding a point to a PPP. Therefore, without loss of generality, we perform the analysis for the typical link whose destination and source are placed at the origin and $\mathbf{x}_o \equiv [R, 0]$, respectively. The signal-to-interference ratio (SIR) measured at the typical destination in the n-th transmission slot is

$$\mathtt{SIR}_n = \frac{h_{\mathbf{x}_o,n} R^{-\alpha}}{\sum_{\mathbf{x}\in\Phi} h_{\mathbf{x},n}\|\mathbf{x}\|^{-\alpha}\mathbf{1}(\mathbf{x}\in\Phi_n)}, \tag{1}$$

where Φ_n is the set of sources with active transmission during the n-th slot, α is the path-loss exponent, and $h_{\mathbf{x},n}$ is channel coefficient from the source at $\mathbf{x}$ during n-th slot. Assuming quasi static Rayleigh fading, we model $h_{\mathbf{x},n} \sim \exp(1)$ independent across both $\mathbf{x}$ and n.

Conditional success probability: The transmission is considered to be successful when the received SIR is greater than a threshold β. From (1), it is quite clear that the successful transmission probability measured at the typical destination placed at o depends on the PPP Φ of interfering sources and is given by $\mu_\Phi = \mathbb{P}[\mathtt{SIR}_n > \beta|\Phi]$

$$\begin{aligned}
&= \mathbb{P}\left[h_{\mathbf{x}_o,n} > \beta R^\alpha \sum\nolimits_{\mathbf{x}\in\Phi} h_{\mathbf{x},n}\|\mathbf{x}\|^{-\alpha}\mathbf{1}(\mathbf{x}\in\Phi_n)\big|\Phi\right],\\
&= \mathbb{E}\left[\exp\left(-\beta R^\alpha \sum\nolimits_{\mathbf{x}\in\Phi} h_{\mathbf{x},n}\|\mathbf{x}\|^{-\alpha}\mathbf{1}(\mathbf{x}\in\Phi_n)\right)\big|\Phi\right],\\
&\overset{(a)}{=} \prod_{\mathbf{x}\in\Phi} \frac{p_{\mathbf{x}}}{1+\beta R^\alpha\|\mathbf{x}\|^{-\alpha}} + (1-p_{\mathbf{x}}),
\end{aligned} \tag{2}$$

where Step (a) follows using the Laplace transform of exponential distribution of $h_{\mathbf{x},n}$, the independence of $\{h_{\mathbf{x},n}, \forall \mathbf{x}, n\}$, and the activity probability $p_{\mathbf{x}}$ of the source at $\mathbf{x} \in \Phi$. In (2), the activities of sources are assumed to be independent. This assumption is necessary for the spatio-temporal analysis, which will be discussed shortly. Note that μ_Φ directly governs packet delivery rate at the typical destination for a given Φ. Unconditioning of μ_Φ w.r.t Φ makes the packet delivery at the typical destination random. Therefore, the knowledge of the distribution of μ_Φ, termed *meta distribution* [21], is crucial to characterize the distribution of the temporal mean AoI.

Traffic model and AoI metric: We consider that sources transmit updates to their corresponding destinations regarding some random processes. The updates of these random processes are assumed to arrive at the sources independently according to a Bernoulli process with parameter $\lambda_{\rm a}$. The links in the close vicinity of each other may experience arbitrarily small update delivery rate because of severe interference, especially when update arrival rate is high. Therefore, to alleviate the impact of severe interference in such cases, we assume that each source attempts transmission with probability ξ independently of the other sources in a given time slot. Also note that the probability of the attempted transmission being successful in a given time slot is equal to μ_Φ because of the assumption of independent fading. Therefore, the number of slots needed for delivering an update at the typical destination can be modeled using the geometric distribution with parameter $\xi\mu_\Phi$ for a given Φ.

This paper considers that each source only stores its latest update arrival since storing and sending older packets does not reduce AoI at its destination [13]. Therefore, the updates arriving during transmission of the ongoing update delivery are simply dropped.For this queue discipline, our aim is to characterize the timeliness of random process $H_{\mathbf{x}}(t)$ observed by the source $\mathbf{x} \in \Phi$ at its corresponding destination using AoI. Let t_k and t'_k be the time instances of the arrival and reception of the k-th update at the source and destination, respectively. For time slot n, let $D_n = \max\{k|t'_k \le n\}$ be the slot index of the most recent update at the destination and A_n be the slot index of the arrival (at source) of the most recent update received at destination (i.e., at D_n). The AoI is defined as

$$\Delta(n) = \begin{cases} \Delta(n-1)+1, & \text{if transmission fails} \\ \Delta(n-1)+1+A_n, & \text{otherwise.} \end{cases} \tag{3}$$

The AoI $\Delta(n)$ increases in a staircase fashion and drops upon reception of a new update at the destination to the total time experienced by this new update in the system. Note that the minimum possible AoI is one because of the arrival and delivery of an update are considered to be at the beginning and end of transmission slots. Now, we formally define peak AoI, which will be studied in detail in this paper.

Definition 1 (Peak AoI)**.** *The peak AoI is defined in [22] as the value of AoI process $\Delta(n)$ measured immediately before the reception the k-th update and is given by*

$$A_k = T_{k-1} + Y_k. \tag{4}$$

where $T_k = t'_k - t_k$ and $Y_k = t'_k - t'_{k-1}$.

The mean peak AoI measured at the typical destination depends on the conditional success probability μ_Φ and hence the mean peak AoI is a random variable. Therefore, our goal is to determine the distribution of the conditional mean peak AoI of the SD pairs distributed across the network. In the following we define the distribution of mean peak AoI.

Definition 2. *Let $\bar{A}(\beta;\Phi) = \mathbb{E}[A_k|\beta;\Phi]$ denote the conditional (temporal) mean peak AoI measured at the typical destination for given Φ and SIR threshold β. The cumulative distribution function (CDF) of $\bar{A}(\beta;\Phi)$ is defined as*

$$F(x;\beta) = \mathbb{P}[\bar{A}(\beta;\Phi) \le x]. \tag{5}$$

III. Analysis of the Peak AoI

The sample path of the AoI process is illustrated in Fig. 1. The red upward (blue downward) marks indicate the arrival

(reception) of updates at the source (destination). The red cross marks indicate the instances of dropped updates which arrive while the server is busy. We first derive the conditional mean peak AoI $\bar{A}(\beta;\Phi)$ in the following subsection and then we present an approach to derive the distribution of $\bar{A}(\beta;\Phi)$ using stochastic geometry in the subsequent subsections.

A. Conditional Mean Peak AoI

The update delivery rate is governed by the product of the medium access probability ξ and the conditional success probability μ_Φ. The mean number of slots required for successful transmission of an update, given Φ, is $\mathbb{E}[T_k] = \xi^{-1}\mu_\Phi^{-1}$. Since

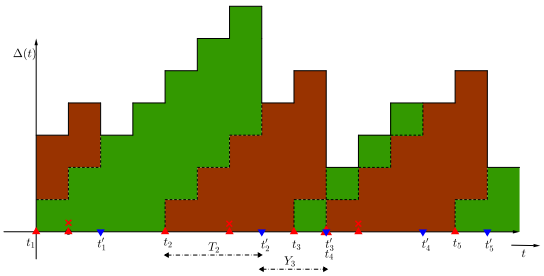

Figure 1. Typical illustration of a sample path of the AoI $\Delta(n)$.

we assumed zero length buffer queue, the next transmission is possible only for the update arriving after the successful reception of the ongoing update. Therefore, the time between the successful reception of $(k-1)$-th and k-th updates is

$$Y_k = S_k + T_k,$$

where S_k is the number of slots required for the k-th update to arrive after the delivery of the $(k-1)$-th update. Since the transmission of the next new update (after successful delivery) begins in the same slot it arrives, we have $S_k \geq 0$. Thus, the pmf of S_k can be modeled using a geometric distribution with parameter $\lambda'_{\mathrm{a}} = \lambda_{\mathrm{a}}/(1-\lambda_{\mathrm{a}})$. Thus, we get $\mathbb{E}[S_k] = \mathcal{Z}_{\mathrm{a}} = \lambda'^{-1}_{\mathrm{a}}$. Therefore, from (4), $\bar{A}(\beta;\Phi)$ is given by

$$\bar{A}(\beta;\Phi) = \mathcal{Z}_{\mathrm{a}} + 2\mu_\Phi^{-1}\xi^{-1}. \tag{6}$$

Using (6) and the distribution of μ_Φ, we can directly determine the distribution of $\bar{A}(\beta;\Phi)$. However, from (2), it can be seen that the knowledge of probability $p_{\mathbf{x}}$ of the interfering source at $\mathbf{x} \in \Phi$ being active is required to determine the distribution of μ_Φ. Thus, we first determine the activity of the typical source for a given μ_Φ, using which the activities of interfering sources are then obtained.

B. Conditional Activity

As we assume that each source attempts transmission independently in a given time slot with probability ξ, the conditional probability of the typical source being active is

$$\zeta_o = \xi\pi_1, \tag{7}$$

where π_1 is the conditional steady state probability that the source have an update. Thus, ζ_o depends on the probability $p_{\mathbf{x}}$ of the interfering source at $\mathbf{x}$ being active through the conditional success probability μ_Φ (see (2)). The steady state distribution of a queue depends on its arrival and departure

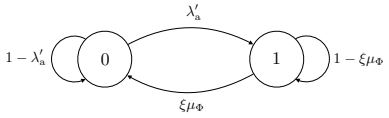

Figure 2. State Diagram where State 0 and State 1 mean that the typical source is idle and busy, respectively.

processes. In our case, both the arrivals and departures of the updates of $H_{\mathbf{x}}(t)$, $\forall \mathbf{x}$, follow geometric distributions with parameters λ'_{a} and $\xi\mu_\Phi$, respectively. Fig. 2 shows the state diagram for the considered queue. The steady state distribution is

$$\pi_0 = \frac{\xi\mu_\Phi}{\lambda'_{\mathrm{a}} + \xi\mu_\Phi} \quad \text{and} \quad \pi_1 = \frac{\lambda'_{\mathrm{a}}}{\lambda'_{\mathrm{a}} + \xi\mu_\Phi} \tag{8}$$

where π_i is the probability of state i.

C. Meta Distribution

It is clear that $\bar{A}(\beta;\Phi)$ jointly depends on the PPP Φ of the interfering sources and their activities $p_{\mathbf{x}}$ through μ_Φ. Hence, the knowledge of the distribution of μ_Φ, i.e., meta distribution, is essential to characterize the spatial distribution of $\bar{A}(\beta;\Phi)$. However, it is very challenging to capture the temporal correlation among the activities of the sources in the success probability analysis. Therefore, we present the moments and approximate distribution of μ_Φ in the following lemma while assuming the activities $p_{\mathbf{x}}$ to be i.i.d.

Lemma 1. *The b-th moment of μ_Φ can be expressed as*

$$M_b = \exp\left(-\pi\lambda_{\mathrm{sd}}\beta^\delta R^2\hat{\delta}C_{\zeta_o}(b)\right), \tag{9}$$

where $\delta = \frac{2}{\alpha}$, $\hat{\delta} = \Gamma(1+\delta)\Gamma(1-\delta)$ and $C_{\zeta_o}(b) = \sum_{m=1}^{\infty}\binom{b}{m}\binom{\delta-1}{m-1}\bar{p}_m$, and $\bar{p}_m$ is the m-th moment of $p_{\mathbf{x}}$. The meta distribution can be approximated with the beta distribution as

$$\mathbb{P}[\mu_\Phi \leq x] \approx I_x(\kappa_1,\kappa_2) \tag{10}$$

where $I_x(\cdot,\cdot)$ is the regularized incomplete beta function and

$$\kappa_1 = \frac{M_1\kappa_2}{1-M_1} \quad \text{and} \quad \kappa_2 = \frac{(M_1-M_2)(1-M_1)}{M_2-M_1^2}. \tag{11}$$

Proof. The b-th moment of μ_Φ given in (2) is

$$M_b = \mathbb{E}_{\Phi,p_{\mathbf{x}}}\left[\prod_{\mathbf{x}\in\Phi}\left(1-\frac{p_{\mathbf{x}}}{1+\beta^{-1}R^{-\alpha}\|\mathbf{x}\|^\alpha}\right)^b\right],$$
$$\overset{(a)}{=} \mathbb{E}_\Phi\left[\prod_{\mathbf{x}\in\Phi}\mathbb{E}_{p_{\mathbf{x}}}\left(1-\frac{p_{\mathbf{x}}}{1+\beta^{-1}R^{-\alpha}\|\mathbf{x}\|^\alpha}\right)^b\right],$$

where Step (a) follows from the assumption of independent activity $p_{\mathbf{x}}$ for $\forall \mathbf{x} \in \Phi$. Now, using the binomial expansion $(1-x)^b = \sum_{m=0}^{\infty}(-1)^m\binom{b}{m}x^m$ for $b \in \mathbb{Z}$, we can write

$$M_b = \mathbb{E}_\Phi\left[\prod_{\mathbf{x}\in\Phi}\sum_{m=0}^{b}(-1)^m\binom{b}{m}\frac{\bar{p}_m}{(1+\beta^{-1}R^{-\alpha}\|\mathbf{x}\|^\alpha)^m}\right],$$

where $\bar{p}_m = \mathbb{E}[p_{\mathbf{x}}^m]$ is the m-th moment of the activity. Using the probability generating functional of PPP Φ and following similar Steps as in [21, Appendix A], we obtain (9). Similar

to [21], the distribution of μ_Φ is approximated using the beta distribution by matching their moments. □

D. Analysis Under Correlated Queues

The activity of a source depends on its successful transmission probability which further depends on the activities of the other sources through interference. Besides, the transmission from this source causes interference to its neighbouring sources which in turn affects their activities. Hence, the successful transmission probabilities of the typical source and its neighbouring sources are correlated through interference which causes coupling in the operations of their queues. It may be noted that the exact analysis of the correlated queues is still an open research problem. Therefore, the usual practice for analyzing such systems is to make meaningful modifications (refer to [23]) so that useful bounds on the network performance can be derived. The readers can refer to [24]–[26] for a small subset of relevant works in the context of wireless networks. On the similar lines of [24], we present a novel two-steps analytical framework to enable an accurate success probability analysis using stochastic geometry while accounting for the temporal correlation in the queues associated with the SD pairs.

• Step 1 (*Dominant System*): For the dominant system, we consider that the interfering sources having no updates transmit dummy updates with probability ξ. As a result, the success probability measured at the typical destination is a lower bound to that in the original system. The b-th moment and approximate distribution of μ_Φ for the dominant system can be evaluated using Lemma 1 by setting $\bar{p}_m = \xi^m$. Using (7), we can obtain the distribution of the activity of the typical source in the dominant system as $\mathbb{P}[\zeta_o \leq t] =$

$$\mathbb{P}\left[\lambda'_{\mathrm{a}}\left(t^{-1}-\xi^{-1}\right) \leq \mu_\Phi\right] \approx 1 - I_{\lambda'_{\mathrm{a}}(t^{-1}-\xi^{-1})}(\kappa_1,\kappa_2) \quad (12)$$

for $0 < t \leq \xi$, where κ_1 and κ_2 are evaluated using (11) by setting $\bar{p}_m = \xi^m$. The m-th moment of the activity of the typical source in the dominant system can be evaluated as

$$\bar{p}^{\mathrm{D}}_m = m\int_0^1 t^{m-1} I_{\lambda'_{\mathrm{a}}\left(\frac{1}{t}-\frac{1}{\xi}\right)}(\kappa_1,\kappa_2)\mathrm{d}t, \quad (13)$$

where κ_1 and κ_2 are obtained using (11) for $\bar{p}_m = \xi^m$.

• Step 2 (*Second Degree of System Modifications*): Similar to [24], we model the activities of the interfering sources independently using the activity distribution of the typical source obtained under Step 1. Thus, similar to Step 1, the b-th moment and the approximate distribution of μ_Φ can be determined using Lemma 1 by setting $\bar{p}_m = \bar{p}^{\mathrm{D}}_m$ given in (13).

E. Moments and Distribution of $\bar{A}(\beta;\Phi)$

Here, we derive the bounds on the moments and distribution of $\bar{A}(\beta;\Phi)$ using the above two-step analysis of μ_Φ.

Theorem 1. *The upper bound of the b-th moment of the conditional mean peak AoI $\bar{A}(\beta;\Phi)$ is*

$$Q_b = \sum_{n=0}^{b}\binom{b}{n}\mathcal{Z}_a^{b-n}2^n\xi^{-n}M_{-n}, \quad (14)$$

where $M_{-n} = \exp\left(-\pi\lambda_{\mathrm{sd}}\beta^\delta R^2\hat{\delta}C_{\zeta_o}(-n)\right)$,

$$C_{\zeta_o}(-n) = \sum_{m=1}^{\infty}\binom{-n}{m}\binom{\delta-1}{m-1}\bar{p}^{\mathrm{D}}_m,$$

and $\bar{p}^{\mathrm{D}}_m$ is given in (13)*.*

Proof. Using (6), the b-th moment of the conditional mean of the peak AoI can be determined as

$$Q_b = \mathbb{E}_\Phi\left[(2(\xi\mu_\Phi)^{-1}+\mathcal{Z}_{\mathrm{a}})^b\right] \overset{(a)}{=} \sum_{n=0}^{b}\binom{b}{n}\mathcal{Z}_{\mathrm{a}}^{b-n}2^n\xi^{-n}M_{-n},$$

where (a) follows using the binomial expansion and $\mathbb{E}[\mu_\Phi^{-n}] = M_{-n}$. According to the Step 2 discussed in Subsection III-D, M_{-n} can be obtained using Lemma 1 by setting $\bar{p}_m = \bar{p}^{\mathrm{D}}_m$. Recall that the two-step analysis provides the lower bound on the success probability μ_Φ because of assuming higher values for activities of the interfering sources. Therefore, the b-th moment of $\bar{A}(\beta;\Phi)$ given in (14) is indeed an upper bound since $\bar{A}(\beta;\Phi)$ is inversely proportional to μ_Φ. □

In the following corollary, we present the simplified expressions for the evaluation of the first two moments of $\bar{A}(\beta;\Phi)$.

Corollary 1. *The upper bound of the first two moments of the conditional mean peak AoI are*

$$Q_1 = \mathcal{Z}_a + 2\xi^{-1}M_{-1} \quad (15)$$

$$Q_2 = \mathcal{Z}_a^2 + 4\mathcal{Z}_a\xi^{-1}M_{-1} + 4\xi^{-2}M_{-2} \quad (16)$$

and the upper bound of its variance is

$$\mathtt{Var} = 4\xi^{-2}\left(M_{-2}-M_{-1}^2\right), \quad (17)$$

where $M_l = \exp\left(-\pi\lambda_{\mathrm{sd}}\beta^\delta R^2\hat{\delta}C_{\zeta_o}(l)\right)$ *and*

$$C_{\zeta_o}(-1) = -\mathbb{E}\left[\zeta_o(1-\zeta_o)^{\delta-1}\right] \text{ and}$$
$$C_{\zeta_o}(-2) = (\delta-1)\mathbb{E}\left[\zeta_o(1-\zeta_o)^{\delta-2}\right] + (\delta+1)C_{\zeta_o}(-1),$$

and distribution of ζ_o is given in (12)*.*

Proof. Solving (14) for $b = \{1,2\}$ and then substituting M_{-1} and M_{-2} from Lemma 1, we obtain (15)-(17). From the definition of $C_{\zeta_o}(b)$, we can directly determine $C_{\zeta_o}(-1) =$

$$\mathbb{E}\Big[\sum_{m=1}^{\infty}\binom{-1}{m}\binom{\delta-1}{m-1}\zeta_o^m\Big] = -\mathbb{E}\left[\zeta_o(1-\zeta_o)^{\delta-1}\right].$$

Now, for $b=-2$, let $C_{\zeta_o}(-2) = \mathbb{E}[B(\zeta_o,-2)]$ where

$$B(\zeta_o,-2) = \sum_{m=1}^{\infty}\binom{-2}{m}\binom{\delta-1}{m-1}\zeta_o^m,$$
$$= \sum_{m=1}^{\infty}(-1)^{2m-1}(m+1)\binom{m-1-\delta}{m-1}\zeta_o^m,$$
$$= -\sum_{m=1}^{\infty}(m-\delta)\frac{\Gamma(m-\delta)}{\Gamma(1-\delta)\Gamma(m)}\zeta_o^m + (\delta+1)\binom{m-1-\delta}{m-1}\zeta_o^m,$$
$$= -\sum_{m=1}^{\infty}\frac{\Gamma(2-\delta)}{\Gamma(2-\delta)}\frac{\Gamma(m-\delta+1)}{\Gamma(1-\delta)\Gamma(m)}\zeta_o^m + (\delta+1)\binom{m-1-\delta}{m-1}\zeta_o^m,$$

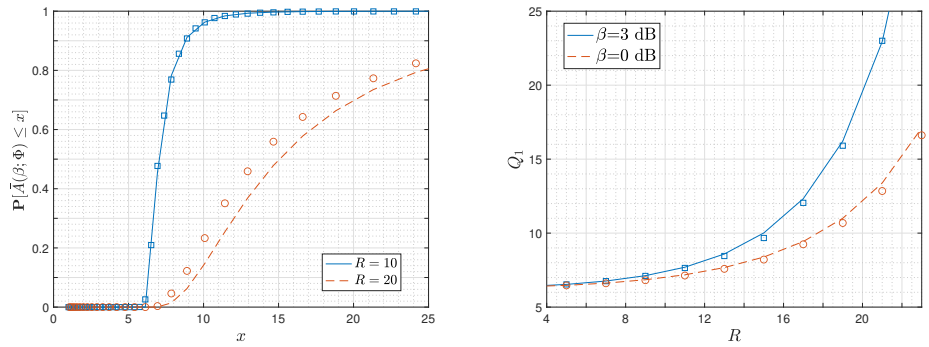

Figure 3. Verification of two-step analytical framework. The curves and markers correspond to the analytical and the simulation results, respectively.

$$= (\delta-1)\zeta_o \sum_{l=0}^{\infty} \binom{l+1-\delta}{l} \zeta_o^l - (\delta+1)\zeta_o \sum_{l=0}^{\infty} \binom{l-\delta}{l} \zeta_o^l,$$
$$= (\delta-1)\zeta_o(1-\zeta_o)^{\delta-2} - (\delta+1)\zeta_o(1-\zeta_o)^{\delta-1}.$$

Finally, $C_{\zeta_o}(-2)$ follows by averaging $B(\zeta_o, -2)$ w.r.t ζ_o. □

Remark 1. *For the mean peak AoI given in* (15)*, the first term captures the impact of the update arrival rate λ_a whereas the second term depends on the inverse mean of the conditional success probability, which captures the impact of wireless link parameters such as the link distance R, network density $\lambda_{\rm sd}$, and path-loss exponent α. Furthermore, it is worth noting that the variance of the conditional (temporal) mean AoI is independent of the arrival rate and entirely depends on the link quality parameters. This is because the arrival rate is assumed to be the same for all SD links and it corresponds to the additive term in conditional mean peak AoI given in* (6)*.*

Corollary 2. *The lower bound of the distribution of the* CDF *of the temporal mean peak AoI is*

$$F_{\rm lb}(x;\beta) = 1 - I_{2\xi^{-1}(x-\mathcal{Z}_{\rm a})^{-1}}(\kappa_1,\kappa_2), \tag{18}$$

where κ_1 and κ_2 are obtain using (11) *for $\bar{p}_m = \bar{p}_m^{\rm D}$.*

Proof. Using (6) and the beta approximation of the distribution of μ_Φ given in Lemma 1, we can determine the distribution of $\bar{A}(\beta;\Phi)$ as $F(x;\beta) =$

$$\mathbb{P}\left[\mu_\Phi \geq 2\xi^{-1}(x-\mathcal{Z}_{\rm a})^{-1}\right] \leq 1 - I_{2\xi^{-1}(x-\mathcal{Z}_{\rm a})^{-1}}(\kappa_1,\kappa_2),$$

where the last inequality follows from the fact that the distribution of μ_Φ (given in Lemma 1) obtained through the two-step analysis is a lower bound. Recall that the parameters κ_1 and κ_2 need to be determined for $\bar{p}_m = \bar{p}_m^{\rm D}$ to enforce the second degree of system modification as discussed in III-D. □

IV. Numerical Results and Discussion

Before presenting the numerical analysis of the peak AoI, we verify the proposed two-step analytical framework for characterizing the AoI using simulation results. Throughout this section, we consider the system parameter as $\lambda_a = 0.3$ updates/slot, $\lambda_{\rm sd} = 10^{-3}$ links/m^2, $\xi = 0.5$, $R = 10$ m, $\beta = 3$ dB, and $\alpha = 4$ unless mentioned otherwise.

Fig. 3 verifies the proposed analytical framework for $R = 10$ and 20 using simulation results. The curves correspond to the analytical results whereas the markers correspond to the simulation results. Note that $R = 10$ and 20 represent a wide enough range for the link distance when $\lambda_{\rm sd} = 10^{-3}$ links/m^2 (for which the dominant interfering source lies at an average distance of around 15 m). Fig. 3 (left) depicts that the lower bound of distribution of the conditional mean peak AoI obtained using Corollary 2 for $R = 20$ is reasonably close, which gets even closer as the link distance R is decreased. However, the mean of the conditional mean peak AoI, i.e., Q_1, as shown in Fig. 3 (right) is a relatively better match to the simulation results compared to its distributions given in Fig. 3 (left). This is because an additional approximation (beta approximation) is used to obtain the distribution of $\bar{A}(\beta;\Phi)$.

While the impact of link distance R on the peak AoI metric is presented in Fig. 3, we show performance trends of the conditional mean peak AoI $\bar{A}(\beta;\Phi)$ with respect to the other wireless link parameters, namely, the SIR threshold β and the path-loss exponent α, in Fig. 4 (left). It may be noted that the success probability reduces with the increase in β and decrease in α. As a result, the mean of $\bar{A}(\beta;\Phi)$, i.e., Q_1, also naturally degrades with respect to these parameters in the same order. It may be noted that Q_1 increases sharply around the value of β where the success probability approaches to zero, which is expected. On the other hand, Q_1 converges to a constant value as β approaches to zero where the success probability is almost one. In this region, Q_1 only depends on the packet arrival rate $\lambda_{\rm a}$ and medium access probability ξ. For $\lambda_{\rm a} = 0.3$ and $\xi = 0.5$, we can obtain $Q_1 \approx 6.33$ by plugging $\mu_\Phi = 1$ in (6) as can be verified using the figure at β approaching to zero. Further, it can also be observed that the standard deviation of $\bar{A}(\beta;\Phi)$ follow similar trend to that of Q_1 except at $\beta \to 0$.

The average and standard deviation of the conditional mean peak AoI are shown with respect to the medium access probability ξ in Fig. 4 (middle) and the status update arrival rate $\lambda_{\rm a}$ in Fig. 4 (right). From these figures, it can be seen that Q_1 approaches to infinity as $\lambda_{\rm a}$ and/or ξ drop to zero. This is because the expected inter arrival times between updates approach infinity as $\lambda_{\rm a} \to 0$ and the expected delivery time approaches infinity as $\xi \to 0$. On the contrary, increasing $\lambda_{\rm a}$ and ξ reduces the inter-arrival and delivery times of the status updates which causes Q_1 to drop. However, Q_1 again increases with further increase in $\lambda_{\rm a}$ and ξ. This is because the activities of the interfering SD pairs increase significantly at

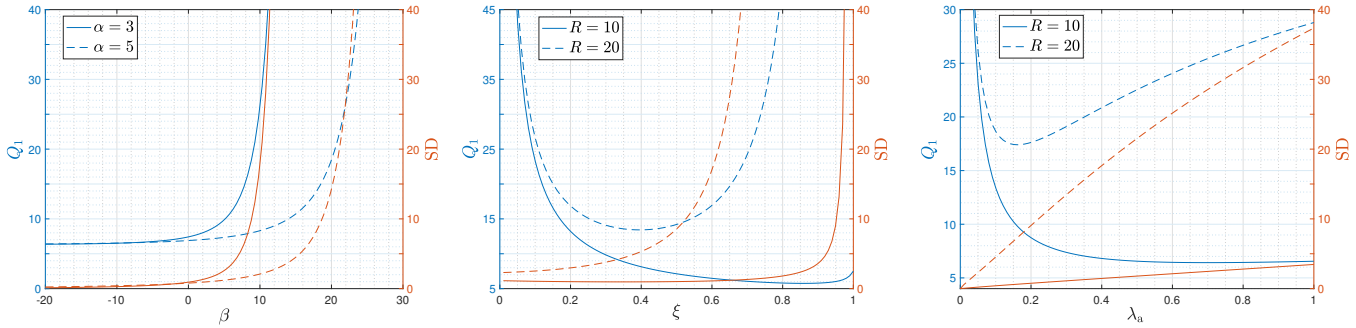

Figure 4. Mean and standard deviation of $\bar{A}(\beta;\Phi)$ versus SIR threshold β (left), medium access probability ξ (middle), and update arrival rate λ_a (right).

higher values of λ_a and ξ, which causes severe interference and hence increase Q_1. Nevertheless, the rate of increase depends on wireless link parameters such as the link distance R, SIR threshold β, path-loss exponent α, etc., which essentially charaterize the success probability. For example, the figure shows that Q_1 increases at faster rate with λ_a and ξ when R is higher (for which the success probability is lower).

V. Conclusion

This paper considered a large-scale wireless network consisting of SD pairs whose locations follow a bipolar PPP. The sources are supposed to keep the information status at their destinations fresh by sending status updates over time. The AoI metric was used to measure the freshness of information. For this system setup, we developed a new stochastic geometry-based approach that allowed us to derive a tight lower bound on the spatial distribution of the temporal mean peak AoI. Our analytical results demonstrated the impact of the update arrival rate as well as the wireless link parameters on the mean and variance of the temporal mean peak AoI. The numerical results revealed that the temporal mean peak AoI can be minimized by appropriately selecting the arrival rate and medium access probability for given system parameters, such as link distance and SIR thresholds.

References

[1] P. D. Mankar, M. A. Abd-Elmagid, and H. S. Dhillon, "Spatial distribution of the mean peak age of information in wireless networks," *IEEE Trans. Wireless Commun.*, to appear.

[2] M. A. Abd-Elmagid, N. Pappas, and H. S. Dhillon, "On the role of age of information in the Internet of things," *IEEE Commun. Magazine*, vol. 57, no. 12, pp. 72–77, 2019.

[3] S. Kaul, R. Yates, and M. Gruteser, "Real-time status: How often should one update?" in *Proc., IEEE INFOCOM*, 2012.

[4] A. Kosta, N. Pappas, and V. Angelakis, "Age of information: A new concept, metric, and tool," *Foundations and Trends in Networking*, vol. 12, no. 3, pp. 162–259, 2017.

[5] I. Kadota, E. Uysal-Biyikoglu, R. Singh, and E. Modiano, "Minimizing the age of information in broadcast wireless networks," in *Proc., Allerton Conf. on Commun., Control, and Computing*, 2016.

[6] M. Bastopcu and S. Ulukus, "Who should google scholar update more often?" in *Proc., IEEE INFOCOM Workshops*, 2020.

[7] B. Buyukates, A. Soysal, and S. Ulukus, "Age of information in Two-hop multicast networks," in *Proc., IEEE Asilomar*, 2018.

[8] M. A. Abd-Elmagid, H. S. Dhillon, and N. Pappas, "A reinforcement learning framework for optimizing age of information in rf-powered communication systems," *IEEE Trans. Commun.*, vol. 68, no. 8, pp. 4747–4760, 2020.

[9] M. K. Abdel-Aziz, C.-F. Liu, S. Samarakoon, M. Bennis, and W. Saad, "Ultra-reliable low-latency vehicular networks: Taming the age of information tail," in *Proc., IEEE Globecom*, 2018.

[10] M. A. Abd-Elmagid and H. S. Dhillon, "Average peak age-of-information minimization in UAV-assisted IoT networks," *IEEE Trans. Veh. Technol.*, vol. 68, no. 2, pp. 2003–2008, Feb. 2019.

[11] M. A. Abd-Elmagid, A. Ferdowsi, H. S. Dhillon, and W. Saad, "Deep reinforcement learning for minimizing age-of-information in UAV-assisted networks," *Proc., IEEE Globecom*, Dec. 2019.

[12] Y. Inoue, H. Masuyama, T. Takine, and T. Tanaka, "A general formula for the stationary distribution of the age of information and its application to single-server queues," *IEEE Trans. Info. Theory*, vol. 65, no. 12, pp. 8305–8324, 2019.

[13] J. P. Champati, H. Al-Zubaidy, and J. Gross, "On the distribution of aoi for the GI/GI/1/1 and GI/GI/1/2* systems: Exact expressions and bounds," in *Proc., IEEE INFOCOM*, 2019.

[14] O. Ayan, H. M. Gürsu, A. Papa, and W. Kellerer, "Probability analysis of age of information in multi-hop networks," *IEEE Netw. Lett.*, 2020.

[15] A. Kosta, N. Pappas, A. Ephremides, and V. Angelakis, "Non-linear age of information in a discrete time queue: Stationary distribution and average performance analysis," in *IEEE ICC 2020*, 2020, pp. 1–6.

[16] M. Haenggi, *Stochastic geometry for wireless networks*. Cambridge University Press, 2012.

[17] Y. Hu, Y. Zhong, and W. Zhang, "Age of information in Poisson networks," in *Proc., IEEE WCSP*, 2018.

[18] H. H. Yang, A. Arafa, T. Q. Quek, and V. Poor, "Optimizing information freshness in wireless networks: A stochastic geometry approach," *IEEE Trans. Mobile Comput.*, [Early Access].

[19] M. Emara, H. Elsawy, and G. Bauch, "A spatiotemporal model for peak AoI in uplink iot networks: Time versus event-triggered traffic," *IEEE Int. Things J.*, vol. 7, no. 8, pp. 6762–6777, 2020.

[20] P. D. Mankar, Z. Chen, M. A. Abd-Elmagid, N. Pappas, and H. S. Dhillon, "Throughput and age of information in a cellular-based IoT network," 2020, available online: arxiv.org/abs/2005.09547.

[21] M. Haenggi, "The meta distribution of the SIR in Poisson bipolar and cellular networks," *IEEE Trans. Wireless Commun.*, vol. 15, no. 4, pp. 2577–2589, 2016.

[22] M. Costa, M. Codreanu, and A. Ephremides, "On the age of information in status update systems with packet management," *IEEE Trans. Inf. Theory*, vol. 62, no. 4, pp. 1897–1910, 2016.

[23] R. R. Rao and A. Ephremides, "On the stability of interacting queues in a multiple-access system," *IEEE Trans. Inf. Theory*, vol. 34, no. 5, pp. 918–930, Sep. 1988.

[24] T. Bonald, S. Borst, N. Hegde, and A. Proutiére, *Wireless data performance in multi-cell scenarios*. ACM, 2004.

[25] Y. Zhong, M. Haenggi, T. Q. S. Quek, and W. Zhang, "On the stability of static Poisson networks under random access," *IEEE Trans. Commun.*, vol. 64, no. 7, pp. 2985–2998, July 2016.

[26] Y. Zhong, T. Q. S. Quek, and X. Ge, "Heterogeneous cellular networks with spatio-temporal traffic: Delay analysis and scheduling," *IEEE JSAC*, vol. 35, no. 6, pp. 1373–1386, 2017.